Near Surface Geophysics, 2003, 77-84

Geophysical study of an landslide in northern Sicily

P. Cosentino*, R. Martorana, M. Perniciaro and L.M. Terranova

Via Archirafi 26, 90123 Palermo, Italy

Received November 2001, revision accepted November 2002

ABSTRACT

The San Fratello area in the Nebrodi Mountains (northern Sicily) is a region of high instability. It has suffered many devastating occurrences, which have hit and destroyed the village of San Fratello. At present the area is still subject to a high landslide risk.

A series of geophysical surveys have been carried out with the aim of determining the thickness and dimensions of the landslide body as well as some tectonic features, in order to gain insight into the evolution of the landslide. The following geophysical techniques have been used: borehole seismic tomography, i.e. down-hole tomographic seismic soundings (DH TSS), time-domain electromagnetic (TDEM) soundings and georadar profiling (GPR). An additional objective was to compare the efficiency of the geophysical methods used in real geological, morphological and logistic situations.

The data obtained using seismic tomography outlined the shape and the thickness of the body of the landslide in the scar and track area, as well as some mechanical characteristics of the formations involved in the movement. TDEM soundings provided a little additional information on the upper 5–10 m. Georadar profiles supplied some information about the locations of some lateral lithological changes.

Finally the information obtained with the various geophysical techniques was used to provide an outline of the history of the area.

INTRODUCTION

The area studied is located in the north-eastern Sicilian chain (the Nebrodi Mountains). It consists of fragments of faulted carbonatic rocks (20–50 m thick), quartz-arenites and argillites belonging to various Flysch formations.

Due to instability, over the centuries this area has suffered many devastating landslides that have hit and destroyed the village of San Fratello. Information about landslides in this area was first obtained in the 18th century (Amico 1757) and includes events up to the last century (Crinò 1921, 1922). In the biggest event, on January 8th 1922, the landslide affected the whole of the centre of San Fratello, when an upper escarpment was formed in the centre of the village for a length of about 600 m and a height of about 40 m. The whole length of the landslide was more than 3000 m and the maximum width was approximately 900 m, the maximum thickness being evaluated at about 70 m (Bellitto *et al*. 1995). This landslide destroyed more than 1000 houses and reached the Furiano River, where it formed a barrage.

The next rotational slide occurred in 1963, with a back movement of the crown area. Then in January 1977, after a period of very high rainfall and floods, renewed movement of a previous slide struck the areas of Polezzo and Pedicitore (Bellitto *et al.* 1995). At present there is still intense activity in the area, due to gravitational (and perhaps also tectonic) stresses, so that the built-up area is subject to a high landslide risk.

From a geological point of view (Fig. 1), the area consists of overlying tectonic units forming the southern part of the Apennine-Maghrebian Chain. Such units are the final result of the south-vergent Langhian-Tortonian overthrust process. In the area of San Fratello, units belonging to both the Sicilian and the Calabrian Complexes are exposed.

The Sicilian Complex succession consists of:

- alternating foliated argillites and poorly graded quartzarenites, having a thickness of about 1 m (Mount Soro Flysch, quartzarenitic member);
- alternating foliated argillites and calcilutites and calcarenites having a thickness of about 20 cm (Mount Soro Flysch, carbonatic member).

The Mount Soro Flysch is unconformably overlain by the terrains of the Longi-Taormina unit (Calabrian domain). This unit, probably allochthonous with respect to the underlying argillites, is composed of different thrusting

* pietro.cosentino@unipa.it

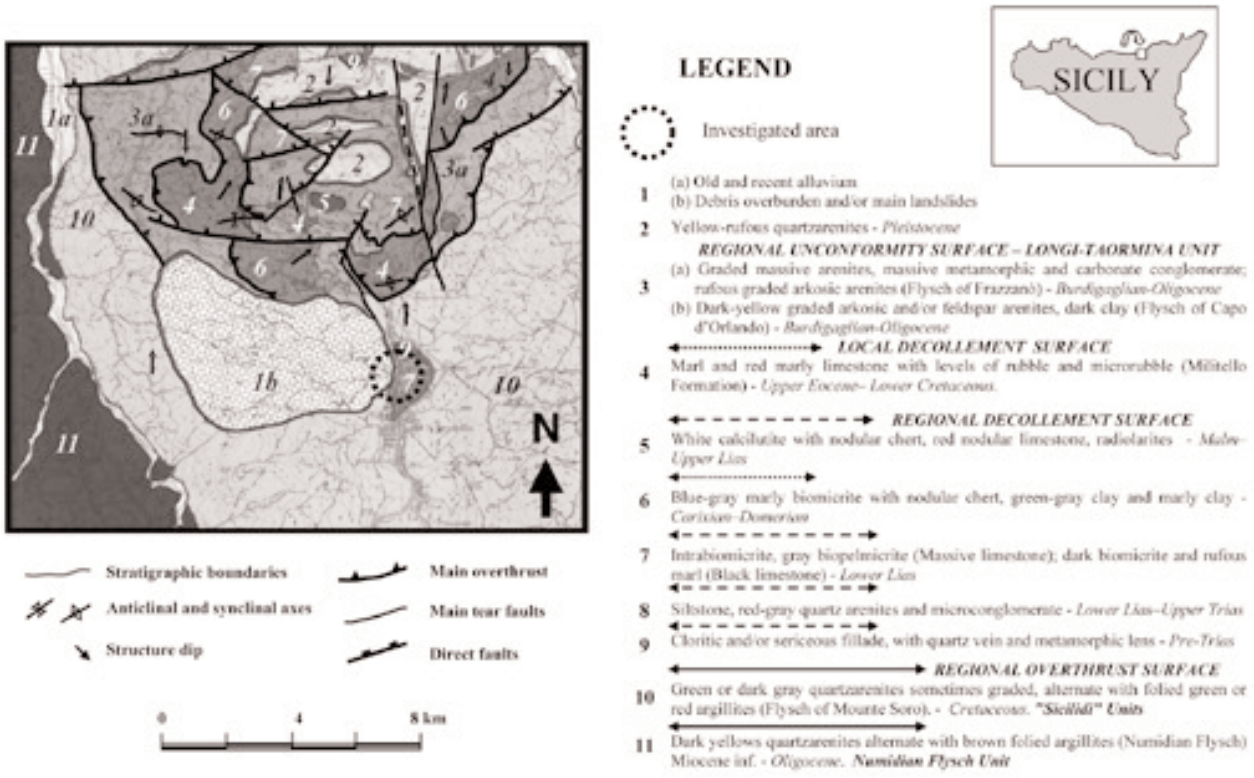

FIGURE 1
Geological sketch of the area of San Fratello village (after Nigro 1994, modified).

units of lower order. Its oldest part, representing the Palaeozoic igneous basement (Truillet 1968), consists of light-grey fillades (sometime graphitose), lenses of dark-grey limestones and sericitic green semi-schists.

In the basement, which has a tectonic discontinuity, arenites and continental quartzitic microconglomerates are present. These sediments (lower Lias age) have a thickness of about 1 m, and they are associated with rufous argillites.

Another tectonic contact connects upper Lias calcareous marls, Dogger-Malm nodular limestones and Cretaceous-Eocene marly limestones. Finally the Frazzanò Flysch (argillites and arkosic arenites) lies on the top of the succession.

The Longi-Taormina unit is intersected by fault and fold systems, which have dislocated all the various formations, giving rise to a very irregular geometrical framework.

The relief of the village of San Fratello is composed of lower-Lias limestone, overthrusting the argillites of Mount Soro. This relief extends in a north-south direction and is delimited by two streams: the Inganno to the east and the Furiano to the west. The area has been affected by complicated gravitational processes, which have produced a morphology characterized by slopes, steps, reverse gradients and hollows.

The planimetric development of the area reflects the typical structures of an extremely complicated gravitational process: buildings and roads often encircle the crown areas and detachment niches of lower landslides (Bellitto *et al.* 1995).

Both slopes of the crest on which San Fratello is situated have been demolished by landslides. On the western slope, gravitational deformation as well as various morphogenetic processes, and also the presence of a superficial aquifer located between the limestones and argillites, have produced massive devastation. This is due to the quartzarenitic blocks, which were produced by tipping phenomena (Carrara *et al.* 1985). They then crumbled, thus causing the regression of the niches.

The carbonatic portions float on the argillites, consequently establishing *lateral spreading* phenomena (Carrara *et al.* 1985).

Various elements contribute to the main characteristics of this landslide, which can be described as a rotational slide associated with mud flow (Carrara *et al.* 1985): (1) the large extent of the landslide; (2) the presence of various locations characterized by reverse gradients; (3) the steps in concordant and reverse directions to the slope; (4) the hollows and depression along the slope.

From a preliminary study (including a topographic survey, drillings, tiltmeter measurements, strain gauge

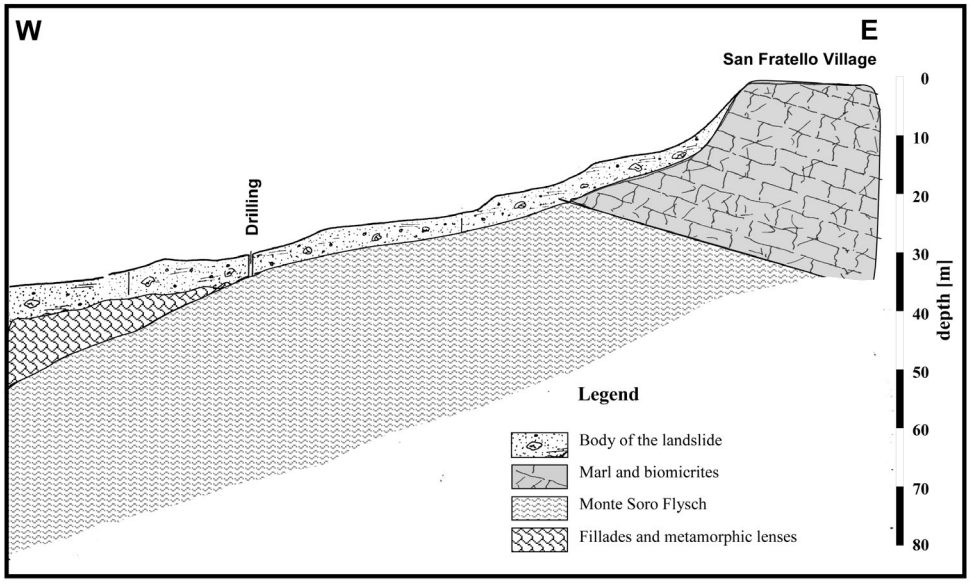

FIGURE 2
A rough sketch of a section along the slope of the landslide, as determined from preliminary studies. The trace of the section is along the W-E direction within the investigated area (circle in Fig. 1). The same scale is used for depths and distances.

measurements), we have been able to make an initial outline of the landslide, illustrated by the dipping section (along the slope direction) in Fig. 2.

THE GEOPHYSICAL PROJECT

At the request of the regional authority, a geophysical survey was carried out in the crown zone and in the body of the landslide to determine aspects of the geometry of the rocks involved in the movement, as well as to evaluate the physical characteristics of these rocks.

The geophysical survey included several different methodologies to test their feasibility and applicability under real geological and morphological conditions, as well as in the framework of a difficult logistic, urban situation. In particular the following surveys were carried out:

- Four borehole DH tomographic seismic profiles in four different directions (the deep ones used 48 hydrophones and 56 seismic sources, while the shallow ones used 24 hydrophones and 28 seismic sources). The apparatus used was an ABEM Terraloc Mark 6; the hydrophones were 30-Hz Mark geophones embedded in an impermeable capsule. A 'Minibang' gun provided the seismic sources, in addition to a stacking procedure of two or three shots for greater distances.

During the drilling of the boreholes, the continuously extracted specimens were analysed and studied. The locations of the four boreholes are shown in Fig. 3, in which the shooting directions are also indicated, the shot points being spaced in pseudo-logarithmic arrays.

Non-automatic semi-standard procedures were used for the picking of the seismic signals, which in general had irregular tracks.

Assuming linear raypaths, the 2D tomographic inversion was carried out following the method of Paige and Saunders (1982). Furthermore, for each borehole, a one-dimensional inversion was carried out, using the whole set of experimental data acquired along the various directions (only the results obtained in the central parts of the tomographic sections were used, to avoid the inclusion of outlying pixels).

- Four TDEM soundings, using a ZONGE 3-kW transmitter and a GDP32 6-channel receiver. The coils were square and, because the soundings were made in the village area and also due to logistic reasons, the maximum size of the wedge was limited to 13 m. A coincident loop array was used, following the method of Nabighian and Macnae (1991).

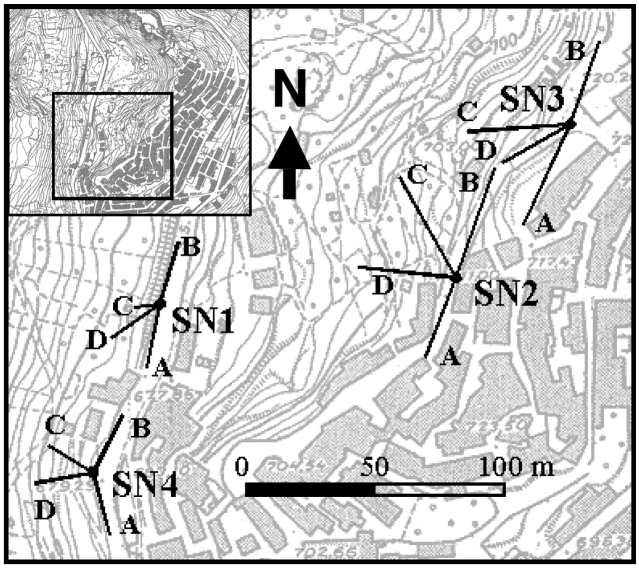

FIGURE 3
Locations of the DH TSS carried out in the area.

The experimental decay data were collected using five different energy conditions, in particular a square wave with null phase. Several frequencies of the square wave were used to obtain the different decay times, namely 2, 4, 8, 16 and 32 Hz.

The values of the apparent resistivity (late time) were then used for interpretation using 1D models. The locations of the EM soundings (TEM 1–TEM 4) are shown in Fig. 4.
- 600 m of GPR profiles using 100 MHz and 40 MHz antennae. A value of 6.0 was assumed for the mean dielectric constant used to obtain the depth of the reflections (the calibration was carried out with some previously obtained stratigraphic sections). The traces of all the GPR profiles are shown in Fig. 5.

Borehole seismic tomography (down-hole tomographic seismic sounding)

The inversion of the tomographic seismic sections was carried out using a back-projection of the experimental traveltime data. A 2D model with linear raypaths, as in a homogeneous earth, was used in the directions investigated.

The main differences between the tomographic sections obtained and the 'real situation' can be summarized as follows:
1. In the sections the values of the velocities are more homogeneous than in reality, since the contrasts between the slow and fast zones are smoothed and thus the velocity gradients are also smoothed.
2. In turn, the shapes of the structures appear smoothed. Consequently the geometrical features should be filtered using a special deconvolution with the 'geological sketch' that best exemplifies the landslide structure.

A general test and calibration were carried out using some values from various sections pertaining to the central part around the borehole, where the trend was regular. These values were integrated for each borehole, to obtain a 'one-dimensional' model.

To construct such model all the irregularities were filtered out (for instance, those due to high velocities because of cementation of the walls of the borehole).

The model obtained in this way (Fig. 6) agreed quite well with the results obtained from geotechnical logging.

A selected set of tomographic sections is shown in Figs 7–12. The behaviour of the velocity is represented, after a smoothing interpolation, on a grey scale.

For borehole SN1, the profile in the directions A and B (Fig. 7, left side) shows low velocities (somewhat higher than 1000 m/s) down to a depth of about 8 m. Two further low-velocity zones are located at 10 m (direction A) and about 13 m (direction B): they show shallow weakness zones. Along the profiles in the C and D directions (Fig. 8), the velocity values are still lower, probably due to large

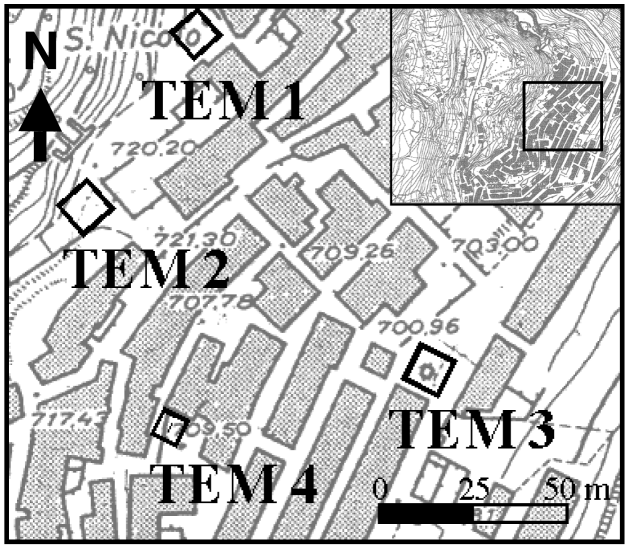

FIGURE 4
Locations of the TDEM soundings carried out in the area.

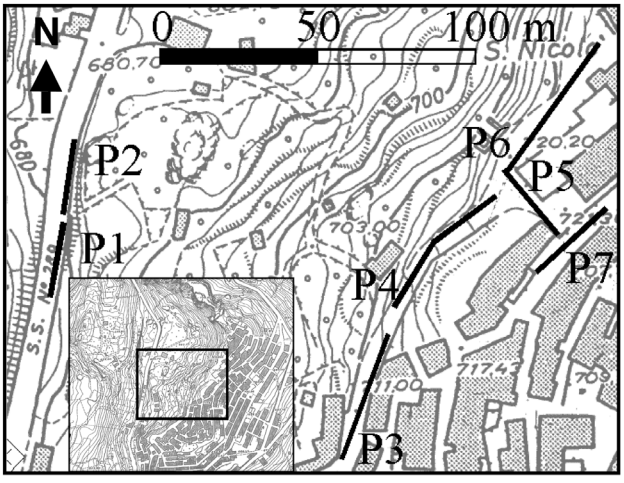

FIGURE 5
Locations of the GPR profiles acquired in the area.

steps in underlying gabions, which interrupt some seismic rays. At greater depths, higher velocity values (about 1400 m/s) represent more consistent layers.

For borehole SN4, not far from borehole SN1, the profile shows high velocity values in the directions A and B (Fig. 7, right side), but along the declivity (directions C and D, Fig. 9), the velocity values are still lower than those obtained from borehole SN1, under the same slope conditions.

In addition this borehole shows a large difference between the profiles roughly parallel and perpendicular to the slope. Along the declivity, the slope-breaks can lower the values of the apparent velocity. At deeper levels, the

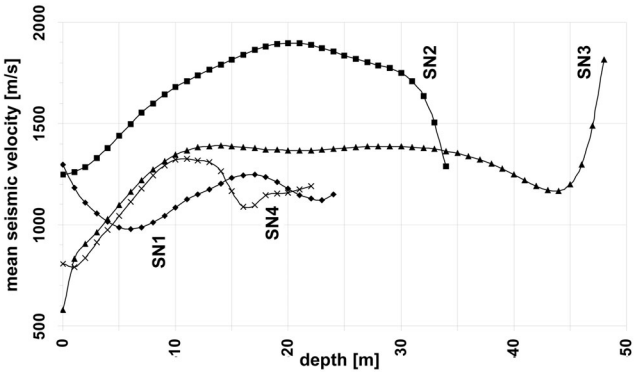

FIGURE 6
Model obtained from DH TSS carried out in the area.

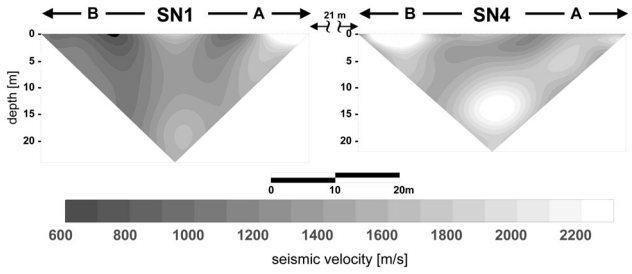

FIGURE 7
2D profiles obtained from DH TSS carried out using borehole SN1 (along B and A directions) and borehole SN4 (along B and A directions).

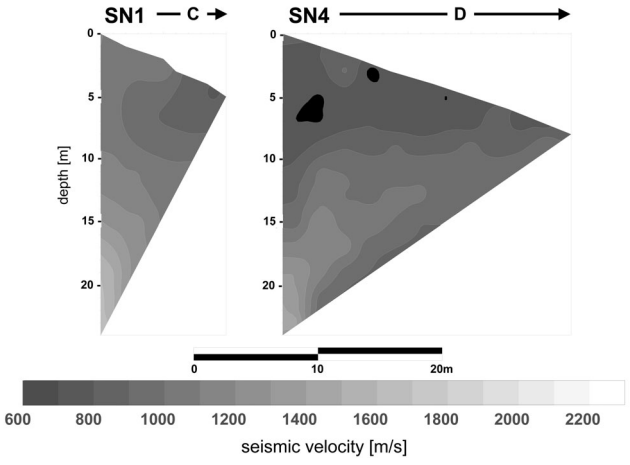

FIGURE 8
2D profiles obtained from DH TSS carried out using borehole SN1, along C (left) and D (right) directions.

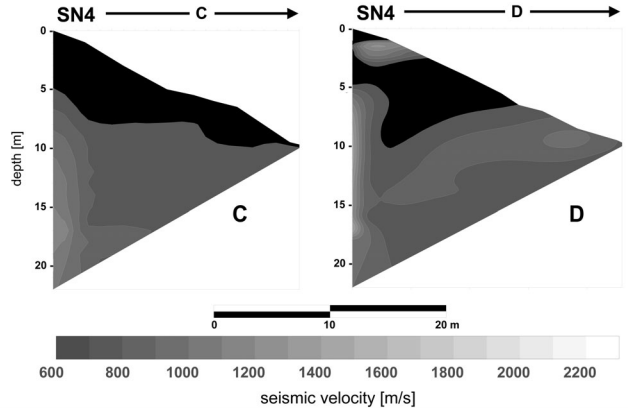

FIGURE 9
2D profiles obtained from DH TSS carried out using borehole SN4, along C (left) and D (right) directions.

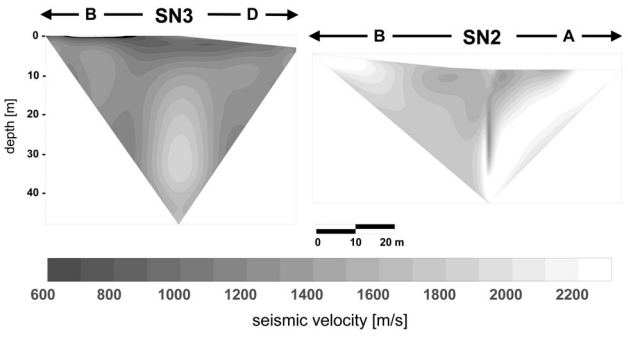

FIGURE 10
2D profiles obtained from DH TSS carried out using borehole SN3 (along B and D directions) and borehole SN2 (along B and A directions).

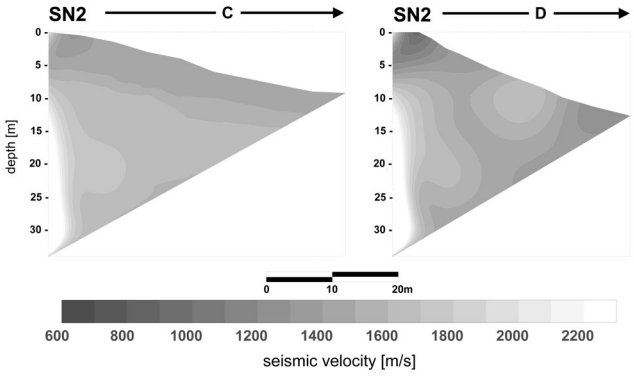

FIGURE 11
2D profiles obtained from DH TSS carried out using borehole SN2, along C (left) and D (right) directions.

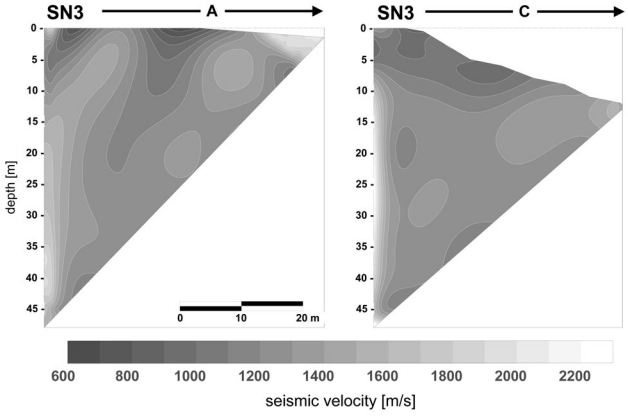

FIGURE 12

2D profiles obtained from DH TSS carried out using borehole SN3, along A (left) and C (right) directions.

velocity increases (about 1700–2000 m/s in the profiles roughly perpendicular to the slope, but much lower in those acquired along-slope).

Figure 7 shows a good agreement between the two parts of the section, and in particular a shallow 'fast' spur in the central part, where a block of limestone is exposed.

Borehole SN2 shows high velocities (about 1400 m/s) in the first metres; the velocity is still increasing (Fig. 10, right side) towards the end of profiles A and B (limestone outcroppings, about 20 m in direction A and about 25 m in direction B). Also in this borehole, the sloping profiles (Fig. 11) show lower velocities, but only for 5–6 m in the first part of the profiles. At increased depths the velocity increases (values ranging from 1500 m/s to over 2000 m/s), which is indicative of more consistent underlying beds.

For borehole SN3, the profiles in all directions (Fig. 10, left side, and Fig. 12), show low but increasing velocities (from 800 m/s to 1250 m/s) in the first 9 m. At greater depths, high velocities (about 1300–1400 m/s, with minor variations along the vertical axis) reveal more consistent beds. Also in Fig. 10 (left side), it is possible to distinguish (in direction B) a very 'slow' shallow layer, where probably the sliding activity in the first few metres is already present.

For borehole SN3, along the profile in direction A (Fig. 12, left side), there are two shallow low-velocity zones (located at about 5 and 23 m). These correspond to weaknesses along the two 'natural' slope-breaks that cut across the profile and are expected to be traces of probable future sliding occurrences.

TDEM soundings

Decay-time data obtained using various square-wave frequencies were compared and used to calculate, after integration and normalization, the values of late-time apparent resistivities against time. The results obtained in terms of a 1D resistivity model are shown in Fig. 13 (TDEM 1 and TDEM 2) and Fig. 14 (TDEM 3 and TDEM 4).

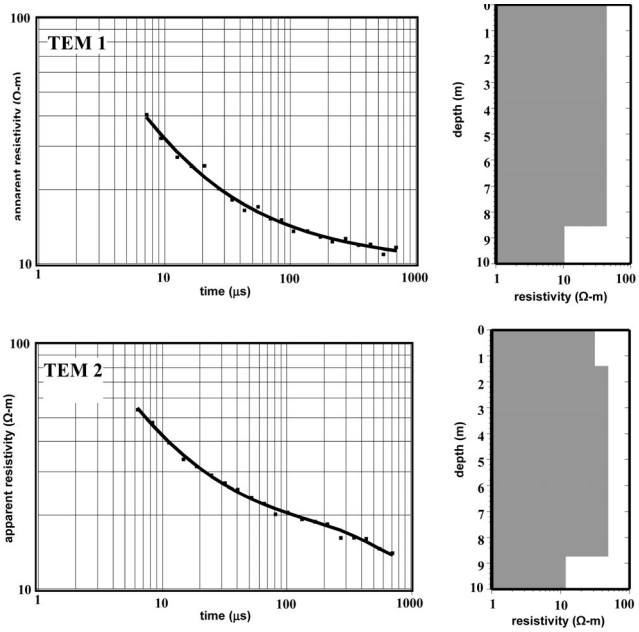

FIGURE 13

Results of the TDEM soundings1 and 2. Graphs of late-time apparent resistivity against time (left) and interpretation in terms of a 1D resistivity model (right).

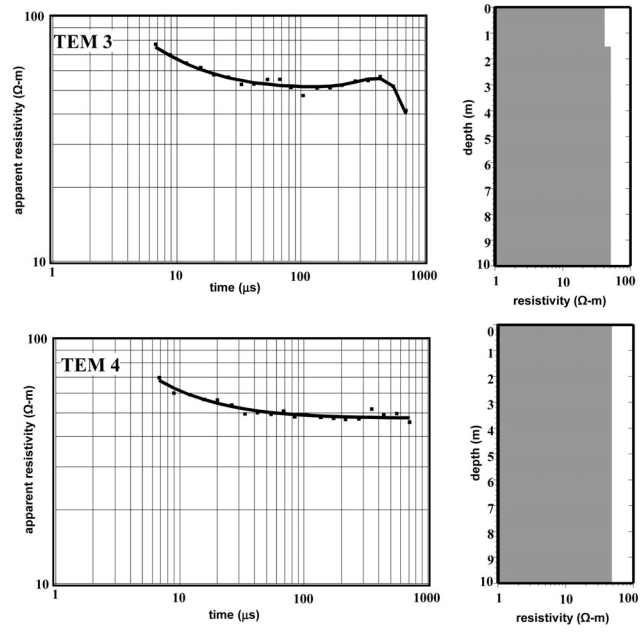

FIGURE 14

Results of the TDEM soundings 3 and 4. Graphs of late-time apparent resistivity against time (left) and interpretation in terms of a 1D resistivity model (right).

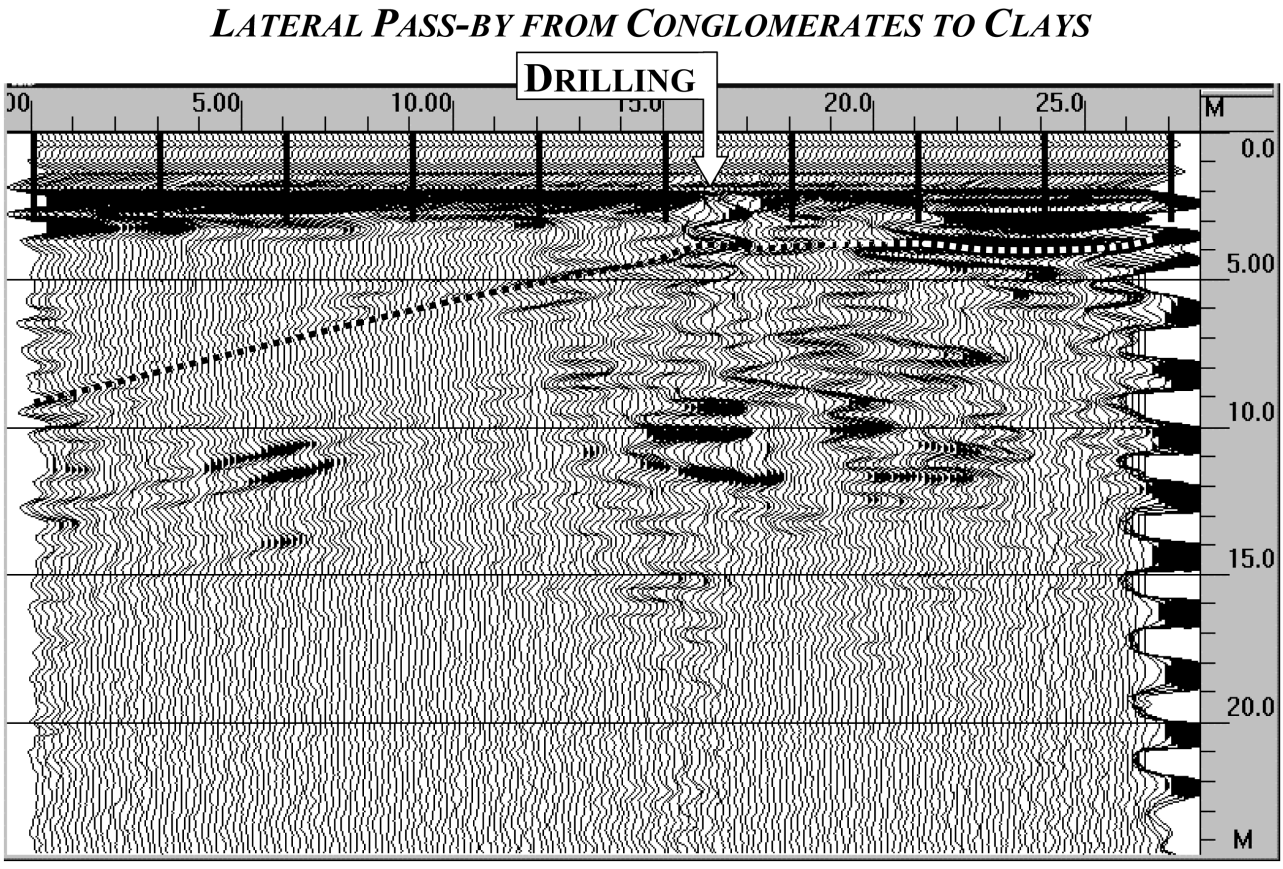

FIGURE 15
GPR profile (P5) in which a lateral by-pass is clearly located.

The electro- and litho-stratigraphies agree sufficiently well with respect to both the layer and thickness parameters of the very shallow terrains. However, the results at depth obtained by means of TDEM soundings appear to be very unsatisfactory. This discrepancy was caused by the inadequate size of the coils, which was limited, due to problems linked with the high density of houses in the village and the presence on the road of cars, motorcycles, tractors and other work vehicles.

Another problem with the quality of the results of the TDEM soundings arises from the large overlap of the resistivity ranges pertaining to the various formations in the shallow layers. In fact, even the autochthonous carbonatic terrains of the lower Lias, such as intrabiomicrite, grey biopelmicrite, dark biomicrite and rufous marl, which in the preliminary phase of the geophysical project had been assigned (from the literature) generally high resistivity values (higher than 500 Ωm), have shown very limited experimental resistivity values (less than 80 Ωm), which are strongly influenced by laterally varying local conditions of water saturation.

GPR profiles

The previously mentioned difficulties due to the overlapping of the resistivity ranges also negatively influenced the GPR survey with regard to (1) a limited penetration depth due to low resistivity values and (2) the difficulty of being able to differentiate between formations characterized by similar resistivities (and dielectric constants).

Nevertheless, along many of the profiles, it is possible to observe the behaviour of some electromagnetic discontinuities and their slope along the acquisition paths. Therefore, along many profiles, some aspects of their complex geology (dip connections, over-thrusting fronts, lateral changes, etc.) were apparently resolved, even if their contribution to the knowledge of the structure of the landslide is small.

Among the various profiles acquired, we selected

profile P5 to be presented in this paper (Fig. 15). It was acquired along a gentle slope in a SE–NW direction. The profile shows a lateral by-pass (also evidenced on the geological survey) from clays to limestones, thus also verifying the presence of a hole (a borehole used for geotechnical logging) along which the stratigraphy is well known.

DISCUSSION AND CONCLUSIONS

The complete set of geophysical results has revealed many aspects of the geometry of the formations involved in the land movement in the area (namely, the thickness of the body of the landslide at different locations, the presence of some points at which detachment is in progress, etc.), as well as some physical properties of the rocks (for instance, differences in velocity, similarities of the elastic parameters).

From a methodological point of view, it is important to note the major contribution that the seismic data makes to the information obtained in comparison with the minor contribution linked to electric and electromagnetic data, at least under these geological, hydrogeological and logistic conditions. Probably, better quality and a larger amount of geoelectric and electromagnetic data are needed to obtain higher resolution.

However, many aspects of the landslide are as yet unknown, namely the influence of the tectonic components from a genetic point of view, and the behaviour of the deep structures (100-–200 m): in the framework of the actual hydrogeological situation, they can regulate the dynamics of the landslide.

In order to investigate these major points, a new project has been proposed. It includes deep investigations with seismic reflection profiles and deep TDEM soundings in the external part of the landslide body, as well as a detailed study of the shallow and deep hydrogeological network.

REFERENCES

Amico V. 1757. Dizionario topografico della Sicilia (translation from Latin by G. Di Marzo, 1855). *Palermo* **1**, 449–451.

Bellitto F., Di Maggio C. and Macaluso T. 1995. Aspetti geomorfologici dei fenomeni di instabilità dei versanti di San Fratello. *Naturalista Sicil*. S. IV, **19** (3-4), 189–205.

Carrara A., D'Elia B. and Semenza E. 1985. Classificazione e nomenclatura dei fenomeni franosi. *Geol. Appl. e Idrogeol.* **20**, II, 223–243.

Crinò S. 1921. Distribuzione geografica delle frane in Sicilia e periodi di maggiore frequenza dei franamenti. *L'Universo, Firenze* II, **6**:447, 1. Carta della distribuzione delle frane 1: 800.000.

Crinò S. 1922. La frana di San Fratello. *Riv. Geogr. It., Firenze* **29**, fasc. 1-2, 63–66.

Nabighian, M.N. and Macnae, J.C., 1991. Time-domain electromagnetic prospecting methods. In: *Electromagnetic Methods in Applied Geophysics* (ed. M.N. Nabighian), Vol **2A**, pp. 427–520. Society of Exploration Geophysicists, Tulsa.

Nigro F. 1994. Note illustrative alla carta geologica del settore occidentale di affioramento dell'Unità Longi-Taormina (M.ti Nebrodi, Sicilia NE). *Riv. Min. Sicil.* N. 6 – 1994, 31–42.

Paige C.C. and Saunders A.M. 1982. LSQR: an algorithm for sparse linear equations and sparse least squares. *ACM Transactions on Mathematical Software* **8** (1), 43-71.

Truillet R. 1968. *Étude géologique des Péloritains orientaux Sicile*. PhD thesis, University of Paris, 441.